Large Molecule Therapeutics

Molecular Cancer Therapeutics

Superior Antitumor Activity of a Novel Bispecific Antibody Cotargeting Human Epidermal Growth Factor Receptor 2 and Type I Insulin-like Growth Factor Receptor

Chao Chen[1], Yanyu Zhang[1], Yu Zhang[1], Jingjing Li[1], Sai Wah Tsao[2], and Mei-Yun Zhang[1]

Abstract

The humanized anti-HER2 monoclonal antibody (mAb) trastuzumab (Herceptin; Genentech) effectively inhibits human epidermal growth factor receptor 2 (HER2)-positive breast tumors. However, many patients responding to treatment often develop resistance. Cross-talk between type I insulin–like growth factor receptor (IGF-IR) and HER2 and elevated IGF-IR signaling have been implicated in tumor cell resistance to trastuzumab therapy. Previously, we reported that the anti-IGF-IR mAb m590 inhibits proliferation and migration of breast cancer MCF-7 cells *in vitro*. Here, we generated a "knobs-into-holes" bispecific antibody (Bi-Ab) against HER2 and IGF-IR by engineering trastuzumab and m590. We compared the effects of Bi-Ab treatment *in vitro* and in SKOV-3 HER2- and IGF-IR–overexpressing cancer xenograft mouse model with those of m590 and trastuzumab treatment alone or in combination. Bi-Ab effectively inhibited proliferation of HER2- and IGF-IR–overexpressing ovarian cancer SKOV-3 cells *in vitro* by ablating receptor phosphorylation and downstream PI3K/Akt and mitogen-activated protein kinase signaling. Bi-Ab more effectively inhibited cancer growth in SKOV-3 HER2- and IGF-IR–overexpressing cancer xenograft mouse model than m590 and trastuzumab alone or in combination. Mice bearing SKOV-3 HER2- and IGF-IR–overexpressing xenografts showed extensive and sustainable tumor regression when treated with Bi-Ab. Our results suggest that Bi-Ab has superior antitumor activity compared with monospecific antibodies, and cotargeting HER2 and IGF-IR may be clinically beneficial in minimizing the acquired resistance to trastuzumab therapy. *Mol Cancer Ther; 1–11. ©2013 AACR.*

Introduction

HER2, encoded by the *ErbB2* gene, is a member of the EGFR/ErbB family (1). HER2 is structurally similar to other EGF receptor (EGFR) family members, including HER1 (EGFR, ErbB1), HER3 (ErbB3), and HER4 (ErbB4), and also acts as a receptor tyrosine kinase (RTK). Homodimerization of HER1 and HER4 upon ligand binding activates intrinsic, intracellular protein-tyrosine kinase activity, resulting in receptor autophosphorylation and downstream signaling, including signaling pathways such as, the Phosphoinositide 3-kinase (PI3K), the c-Jun N-terminal kinase (JNK), and the mitogen-activated protein kinase (MAPK), which promote DNA synthesis, cell proliferation, and inhibition of cell apoptosis. HER3 does not have a tyrosine kinase domain, so it transfers signals upon ligand binding through heterodimerization with other EGFR family members that have kinase activity. Unlike HER1, HER3, and HER4, HER2 is unable to bind ligands and form homodimers. However, HER2 possesses tyrosine kinase activity, and seems to be the major signaling partner for EGFR family members through the formation of heteromeric complexes (2). Heterodimerization between two EGFR family members requires ligand binding (3, 4), but the crystal structure of a truncated HER2 ectodomain suggests that HER2 is constitutively in the activated conformation and readily interacts with HER3 mostly and other EGFR family members (5). Overexpression of HER2 promotes ligand-independent formation of a HER2/HER3 receptor complex, a major oncogenic driver in HER2-overexpressing breast tumor cells (6). Cleavage of HER2 by the extracellular protease, ADAM10, produces the HER2 ectodomain and a truncated, constitutively active HER2 receptor (p95HER2) shown to drive carcinogenesis (7). HER2 overexpression is associated with strong activation of the PI3K pathway, which stimulates cell proliferation by activating the protein kinase Akt and downregulating the cyclin-dependent kinase inhibitor, p27 (8). HER2 can also activate the MAPK pathway via interaction with SHC and GRB2 adaptor proteins (9). Overexpression of HER2 was found in breast and ovarian cancers, and

Authors' Affiliations: Departments of [1]Microbiology and [2]Anatomy, Li Ka Shing Faculty of Medicine, The University of Hong Kong, Pokfulam, Hong Kong, China

Corresponding Author: Mei-Yun Zhang, Department of Microbiology, Li Ka Shing Faculty of Medicine, The University of Hong Kong, L5-45, Laboratory Block, 21 Sassoon Road, Pokfulam, Hong Kong, China. Phone: 852-28183685; Fax: 852-28177805; E-mail: zhangmy@hku.hk

doi: 10.1158/1535-7163.MCT-13-0558

associated with cancer metastasis (10–12), poor clinical outcome, and decreased survival rate (13–15).

Type I insulin-like growth factor receptor (IGF-IR) is a tyrosine kinase receptor composed of 2 α subunits and 2 β subunits. Upon binding to either of the two ligands, insulin-like growth factor I (IGF-I) or IGF-II, the extracellular domain of the α chains induces tyrosine autophosphorylation of the β chains in the cytoplasm. This activates the kinase activity of IGF-IR, and triggers downstream signaling via the PI3K/Akt and Ras/MAPK pathways, resulting in increased cell survival and cell proliferation (16, 17). Elevated IGF-IR is found in many tumor malignancies, including breast, prostate, and lung cancers (18, 19). In addition, overexpression of IGF-IR has been associated with disease progression and cancer metastasis (20, 21).

HER2 is a widely used diagnostic marker and validated target for therapy. The humanized anti-HER2 monoclonal antibody (mAb) trastuzumab (Herceptin; Genentech) has been effective in treating HER2-overexpressing breast cancers (22, 23). Binding of trastuzumab to HER2 causes internalization and degradation of the receptor in SKBR3 and MDA453 cells (24). Trastuzumab binds to domain IV of the extracellular segment of HER2, leading to disruption of HER2/HER3 dimerization and ablation of downstream PI3K/Akt signaling (6). Trastuzumab can also inhibit cleavage of HER2 ectodomain in breast cancer cells, thus block the generation of a constitutively active truncated receptor (p95HER2; refs. 7, 25, 26). In addition, Fc-mediated antibody-dependent cell-mediated cytotoxicity (ADCC) may partially contribute to the antitumor activity of trastuzumab *in vivo* (27).

Only 25% to 30% of the patients with breast cancer overexpress HER2, and patients treated with trastuzumab can develop resistance as the disease progresses. Various mechanisms may account for this resistance, which likely involve the PI3K/Akt pathway, including elevated HER2-associated receptors and other receptors (28, 29), cross activation between HER2 and other receptors (30–32), blockage of trastuzumab by membrane-associated glycoproteins such as mucin-4, removal of the trastuzumab epitope by cleavage or loss of HER2 expression, and increased HER2 expression. Accumulating evidence shows that cross-talk between HER2 and IGF-IR, including receptor heterodimerization and transactivation, and elevated IGF-IR signaling are associated with trastuzumab resistance (31, 33–35). Overexpression of IGF-IR in HER2–overexpressing breast cancer cell lines results in trastuzumab resistance *in vitro* (36). Inhibition of IGF-1R activity enhances the response to trastuzumab in HER-2–positive breast cancer cells (37). A phase II clinical trial of patients with HER2-positive breast cancer revealed that overexpression of IGF-IR in the primary tumor was associated with resistance to trastuzumab (38). Therefore, cotargeting IGF-IR and HER2 may be clinically beneficial in minimizing the acquired resistance to trastuzumab therapy.

We previously described a human/mouse chimeric mAb m590 that specifically bound with high affinity to IGF-IR and blocked the binding of IGF-I and IGF-II to IGF-IR. This inhibited ligand-induced phosphorylation of IGF-IR in breast cancer MCF-7 cells (39). In this study, we generated a bispecific antibody (Bi-Ab) by engineering the m590 and trastuzumab, and tested Bi-Ab *in vitro* and in SKOV-3 HER2- and IGF-IR-overexpressing xenograft mouse model. We found that cotargeting HER2 and IGF-IR with Bi-Ab was more effective than targeting HER2 or IGF-IR alone with the monospecific antibodies or cotargeting HER2 and IGF-IR with a combination (Comb) of the two monospecific antibodies in ablating tumor cell proliferation *in vitro* and *in vivo*.

Materials and Methods

Cell lines, antibodies, and chemicals

Breast cancer MCF-7 cells were cultured in Dulbecco's Modified Eagle Medium (Invitrogen) supplemented with 10% heat-inactivated FBS and 1% penicillin/streptomycin. Ovarian cancer SKOV-3 cells were cultured in McCoy's 5A medium (Hyclone) supplemented with 10% heat-inactivated FBS and 1% penicillin/streptomycin. Both MCF-7 and SKOV-3 cell lines were obtained from National Cancer Institute, NIH (Bethesda, MD). No authentication was done by the authors. The following primary mAbs were purchased from Cell Signaling Technology: rabbit anti-Phospho-AKT (Thr308; C31E5E), rabbit anti-Phospho-p44/42 MAPK (ERK1/2; Thr202/Tyr204; D13.14.4E) XP, rabbit anti-Akt (pan; 11E7), rabbit anti-P44/42 MAPK (ERK1/2; 137F5), and rabbit anti-GAPDH mAb (14C10). The secondary antibodies were purchased from Jackson ImmunoResearch. Xenolight D-luciferin was purchased from Caliper Life Sciences.

Expression and purification of recombinant IGF-IR and HER2 ectodomains

The gene encoding the extracellular domain (ectodomain) of IGF-IR was amplified from the pBlueScript-IGF-IR construct P08069 (39), and subcloned into the pSecTag2C vector at the EcoR I and Not I sites. The gene encoding HER2 ectodomain was amplified from SKOV-3 cell line by reverse transcriptase PCR, and subsequently cloned into the pSecTag2A vector at the Xho I and Sfi I sites. Both constructs were confirmed by DNA sequencing. Recombinant ectodomains of IGF-IR and HER2 were produced by transient transfection of 293T cells. Expression in transfectants was enhanced by the transduction of vaccinia virus vTF7.3 encoding bacteriophage T7 RNA polymerase. Seventy-two hours posttransfection, culture supernatants were collected and His-tagged ectodomains purified by immobilized metal affinity chromatography.

Construction of "knobs-into-holes" CH3 variants

The humanized trastuzumab heavy chain variable region and light chain [DrugBank: trastuzumab (DB00072) (BIOD00098, BTD00098)] genes were synthesized and cloned into the mammalian expression plasmid pDR12 containing human immunoglobulin G (IgG)-1 heavy chain genomic DNA constant regions. Two

mutations were introduced in the CH3 domains of pDR12-trastuzumab (T366Y) and pDR12-m590 (Y407T) using a site-directed mutagenesis kit (Stratagene). The primers for the mutagenesis were: T366Y-F: 5′-CCAGGTCAGCCTGTACTGCCTGGTCAAAG-3′, and T366Y-R: 5′-CTTTGACCAGGCAGTACAGGCTGACCTGG-3′; and Y407T-F: 5′-CTCCTTCTTCCTCACCAGCAAGCTCACCG-3′, and Y407T-R: 5′- CGGTGAGCTTGCTGGTGAGGAAGAAGGAG -3′. The mutations were confirmed by DNA sequencing. The resultant plasmids were designated as pDR12-trastuzumab-366 and pDR12-m590-407, respectively.

Expression and purification of trastuzumab and m590, and Bi-Ab

Trastuzumab and m590 were expressed by transient transfection of 293F cells (Invitrogen) with recombinant plasmids pDR12-trastuzumab and pDR12-m590, respectively. Bi-Ab was expressed by transiently cotransfecting 293F cells with pDR12-trastuzumab-366 and pDR12-m590-407 plasmid DNA. Recombinant antibodies were purified from the culture supernatants by protein A (GE Healthcare) affinity purification.

Indirect ELISA

Recombinant ectodomains of IGF-IR or HER2 (2 μg/mL in both cases) were coated on 96-well high-binding ELISA plates at 4°C overnight. The plates were washed and blocked with 3% bovine serum albumin in PBS at 37°C for 2 hours. Two-fold serially diluted mAb trastuzumab or m590 was added to the wells and the bound mAbs were detected by horseradish peroxidase (HRP)-conjugated anti-human Fc as secondary antibody and 3,3′,5,5′-Tetramethylbenzidine (TMB) substrate. Optical density at 450 nm (OD450nm) was measured after color development at room temperature for 30 minutes. In the case of Bi-Ab, recombinant IGF-IR ectodomains were coated on the plates. Following addition of 2-fold serially diluted antibodies and incubation at room temperature for 2 hours, plates were washed and biotinylated HER2 ectodomain (2 μg/mL) was added to each well. Bound HER2 ectodomains were detected by HRP-conjugated streptavidin and TMB substrate.

Western blotting

MCF-7 or SKOV-3 cells in complete medium were seeded in 6-well plates. When cells reached 70% to 80% confluence, they were incubated in serum-free medium overnight. Cells were treated with antibodies for 30 minutes, followed by addition of 1.5 nmol/L IGF-I and further incubation for 30 minutes. Cells were then lysed and 10 μL of cell lysates from each sample was resolved by 12% SDS-PAGE. Once the proteins were transferred, polyvinylidene difluoride membranes were blocked with 5% skim milk in PBS for 30 minutes, incubated with primary antibodies, and then secondary antibodies. The membranes were extensively washed after each incubation step. The Western blot signal was detected by Western Bright ECL-HRP substrate (Advansta).

Flow cytometry

MCF-7 or SKOV-3 cells were detached using enzyme-free cell-disassociation buffer (Invitrogen), washed twice with PBS, and incubated at 4°C for 2 hours with antibodies in fluorescence-activated cell sorting (FACS) buffer (1% FBS in PBS). Cell surface bound antibodies were detected using phycoerythrin conjugated to anti-human Fc by incubation at 4°C for 1 hour followed by washing twice with FACS buffer and fixation with 2% paraformaldehyde in FACS buffer. The stained cells were analyzed with a BD flow cytometer and FlowJo software.

ADCC assay

The flow cytometry-based ADCC assay has been described previously (40). Here, we used SKOV-3 cells as target cells and healthy human volunteers peripheral blood mononuclear cells (PBMC) as effector cells at an E/T ratio of 20/1. Briefly, SKOV-3 cells were stained with PKH-67 and then mixed with antibodies and PBMCs. Following 2 hours of incubation, 7-Aminoactinomycin D (7-AAD) was added to the mixture. Following several washes, the samples were analyzed by FACS AriaIII flow cytometer using BD FACS Diva software. Percentage of cell death was determined by software analysis of four identifiable cell populations, live effector cells (no dye), dead effector cells (7-AAD positive), live target cells (PKH-67 positive), and dead target cells (PKH-67 and 7-AAD double positive). Percentage of ADCC was calculated as [(% experimental lysis − % spontaneous lysis)/(% maximum lysis − % spontaneous lysis)] × 100, in which "% spontaneous lysis" referred to percentage of dead target cells mixed with effectors in the absence of antibodies, and "% maximum lysis" referred to percentage of dead target cells mixed with effectors in the presence of 1% Triton X-100, and "% experimental lysis" referred to percentage of dead target cells mixed with effectors in the presence of antibodies. The assay was performed in duplicate and repeated once. One representative set of data was shown in this report.

Cell proliferation assay

Antibodies were serially diluted in culture medium containing 2% FBS and mixed with equal volume of SKOV-3 cells containing 3 nmol/L IGF-I. Cell/Ab mixtures were then plated onto 96-well cell culture plates with a final concentration of 2,000 cells per well and 1.5 nmol/L IGF-I. The plates were incubated at 37°C with 5% CO_2 for 72 hours, and cell proliferation level was detected by Cell Titer 96 Aqueous Non-Radioactive Cell Proliferation Assay Kit (Promega).

Generation of the luciferase-expressing SKOV-3 stable cell line

293T cells were transiently cotransfected with recombinant plasmid encoding HIV-1 Gag and polymerase

(Gag-pol), Luc-expressing plasmid, and vesicular stomatitis virus (VSV) backbone plasmid at a ratio of 2/2/1 (Gag-pol/Luc/VSV). Thirty-six to 48 hours posttransfection, culture supernatant containing Luc-lentivirus was collected, and equally mixed with fresh culture medium followed by addition of polybrene to a final concentration of 8 μg/mL. Nine milliliters of the mixture were added to SKOV-3 cells seeded in 100 mm dishes and incubated at 37°C for 6 hours in 5% CO2. Three milliliters of culture medium containing 8 μg/mL polybrene were then added to the dish. Following overnight incubation, infection medium was removed and cells cultured in fresh McCoy's 5A medium containing 1 μg/mL puromycin. After three to five passages, limiting dilution was performed and single cell clones were screened by luciferase assay. The single cell clone expressing the highest level of luciferase was expanded and titrated by imaging in a 96-well plate.

Establishment of a breast tumor xenograft mouse model and the mouse study

This study was approved by University of Hong Kong (HKU; Hong Kong, China) Committee on Using Live Animals in Teaching and Research (CULATR # 2514-11). Nude BALB/c female mice, 4–6-weeks-old, were obtained from the Animal Centre of the HKU. To establish a breast cancer xenograft mouse model, a pilot experiment was carried out by subcutaneously injecting different numbers of SKOV3-Luc cells into nude mice and imaging the mice at different time points. The optimal cell numbers that yielded sustainable and increasing luminescence intensity in the regions of interest (ROI) were determined.

The mouse study was carried out as follow: on day 0, SKOV-3-Luc cells were resuspended in plain McCoy's 5A medium and 3 million of the cells were injected subcutaneously into each nude mouse. On day 1, KETAMINE/XYCAZINE/PBS at a ratio of 1/1.2/7.8 were mixed and 40 μL (2.5 μL/g body weight) of the anesthetic mixture was injected subcutaneously into each mouse. D-luciferin (100 μL) at a concentration of 30 mg/mL in Dulbecco's Phosphate-Buffered Saline (DPBS; 5 μl/g body weight) was then injected intraperitoneally into each mouse (each mouse received 150 mg luciferin/kg body weight). About 15 minute after injection, mice were imaged for luminescence intensity in the ROI using Xenogen IVIS 100 *in vivo* imaging system. Mice were then randomized, so that each group of mice had approximately the same average luminescence intensity. Each group had seven mice and a total of four groups were formed corresponding to trastuzumab, m590, Bi-Ab, and Comb treatment conditions. Each antibody (100 μg) or antibody combination (100 μg total) were injected intraperitoneally into each mouse on days 1, 4, 6, and 8. Mouse imaging was repeated on days 4, 6, 8, 11, 15, 25, and 35. A control group had five mice and were not treated with any antibodies after injection of tumor cells, but imaged at the same time with antibody-treated groups.

Results

Bi-Ab cotargets IGF-IR and HER2

We used the "knobs-into-holes" approach to generate an anti-IGF-IR/anti-HER2 hybrid IgG (41–43). A "knob" mutant was created by replacing a threonine with tyrosine (T366Y) in the CH3 domain of trastuzumab. A "hole" mutant was made by replacing a tyrosine with threonine (Y407T) in the CH3 domain of m590. Cotransfection of 293F cells with the "knob" and "hole" plasmids resulted in the production of stable heterodimers that exhibited bispecificity for both HER2 and IGF-IR (Fig. 1). The Bi-Ab bound to recombinant IGF-IR and HER2 ectodomains (Fig. 1C) and to overexpressed, membrane-associated IGF-IR and HER2 on SKOV-3 cells (Fig. 1B and D). Compared with breast cancer MCF-7 cells used in our previous study, ovarian cancer SKOV-3 cells express a high level of HER2 and a modest level of IGF-IR (Fig. 1A). Similar to the two parental antibodies, m590 and trastuzumab, Bi-Ab bound to SKOV-3 in a dose-dependent manner (Fig. 1D). Moreover, flow cytometry analysis revealed that trastuzumab and Bi-Ab have a similar binding profile, which shows two peaks in the histogram (Fig. 1B), suggesting that cell surface HER2 proteins may have multiple conformational or organizational states.

Bi-Ab inhibits receptor phosphorylation and downregulates downstream PI3K/Akt and MAPK signaling

We previously reported that m590 blocked ligand-induced IGF-IR phosphorylation in breast cancer MCF-7 cells (39), and inhibited MCF-7 cell proliferation and migration (44). We extended these findings in this study by analyzing the downstream signaling of IGF-IR. We found that m590 inhibited ligand-induced phosphorylation of Akt and extracellular signal–regulated kinase (ERK) in MCF-7 cells (Fig. 2A), and synergized with trastuzumab in inhibiting ligand-induced Akt phosphorylation in MCF-7 cells (Fig. 2B). Next, we compared the effects of Bi-Ab, m590, and trastuzumab on phosphorylation of IGF-IR in SKOV-3 cells (Fig. 2C) with downstream signaling in MCF-7 (Fig. 2D) and SKOV-3 cells (Fig. 2E) in the presence of ligand (IGF-I) or absence of ligand (Fig. 2F). Both m590 and Bi-Ab inhibited phosphorylation of IGF-IR in SKOV-3 cells compared with nonspecific human IgG control. Treatment with trastuzumab or Comb did not result in decreased levels of phosphorylated IGF-IR in SKOV-3 cells (Fig. 2C). In MCF-7 cells, m590 and Bi-Ab, as well as Comb inhibited ligand-induced phosphorylation of Akt, but only Bi-Ab inhibited ligand-induced phosphorylation of ERK (Fig. 2D). Treatment with trastuzumab slightly enhanced ligand-induced phosphorylation of Akt in MCF-7 cells (Fig. 2D, lane 2). None of the antibodies showed inhibitory effects on ligand-induced phosphorylation of Akt and ERK in SKOV3 cells at the antibody concentration (100 μg/mL) tested (Fig. 2E). When we compared the effects of Bi-Ab, m590, and trastuzumab on phosphorylation of ERK in MCF-7 and

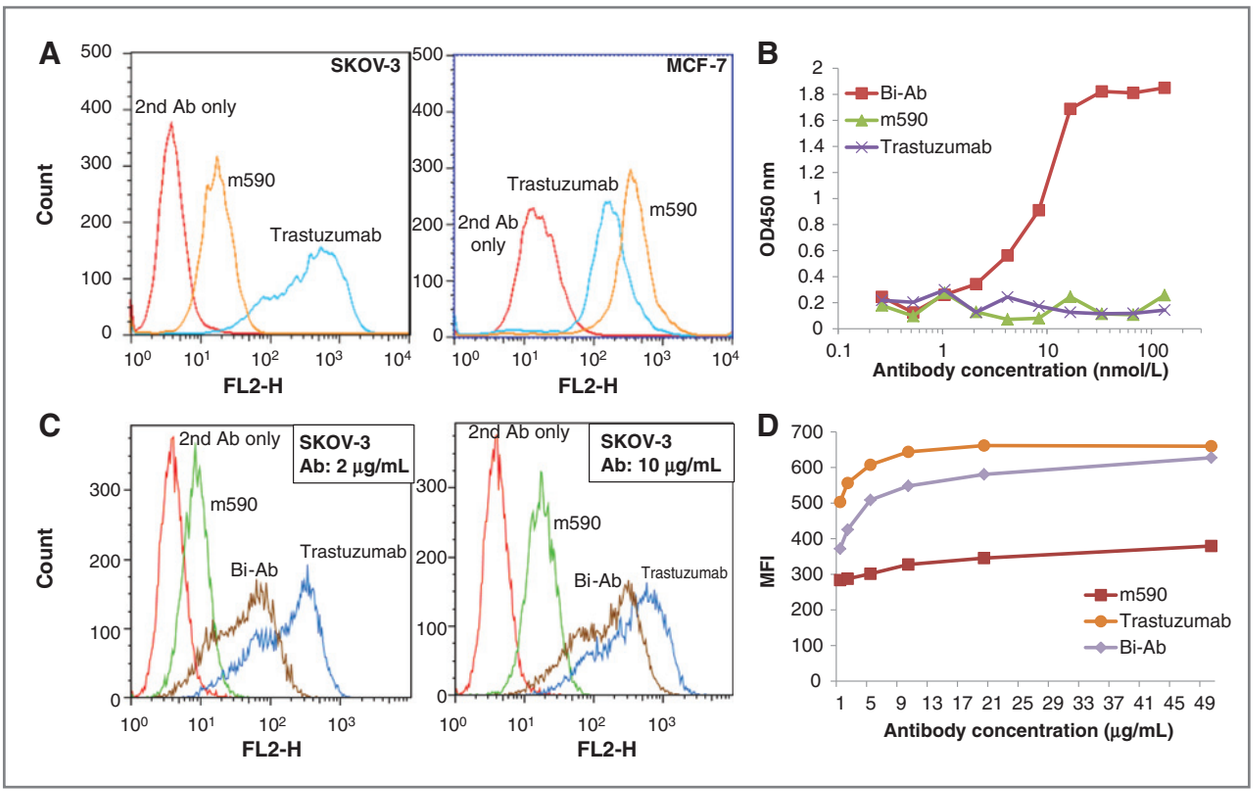

Figure 1. Flow cytometry of SKOV-3 and MCF-7 cells stained with m590 or trastuzumab and characterization of Bi-Ab for binding to recombinant HER2 and IGF-IR ectodomains and membrane-associated HER2 and IGF-IR in comparison with m590 and trastuzumab. A, flow cytometry of breast cancer MCF-7 and ovarian cancer SKOV-3 cells stained with m590 and trastuzumab at 10 μg/mL. B, simultaneous binding of Bi-Ab to recombinant IGF-IR and HER2 ectodomains by indirect ELISA. Recombinant IGF-IR ectodomain was coated in microplates. Three-fold serially diluted Bi-Ab, trastuzumab, and m590 were added to the wells followed by addition of 100 ng per well of biotinylated recombinant HER2 ectodomain. Bound HER2 ectodomain was detected by HRP conjugated to streptavidin and TMB. C, histogram overlay of SKOV-3 cells stained with m590, trastuzumab, and Bi-Ab at 2 and 10 μg/mL. D, binding kinetics of Bi-Ab, m590, and trastuzumab to membrane-associated IGF-IR and HER2 on SKOV-3 cells. Mean fluorescence intensity (MFI) of SKOV-3 cells stained with the antibodies at different concentrations was measured.

SKOV-3 cells (Fig. 2F) in the absence of ligand, we found that in MCF-7 cells, both m590 and Bi-Ab inhibited ERK phosphorylation, and Comb treatment slightly reduced ERK phosphorylation (data not shown), but in SKOV-3 cells, Bi-Ab inhibited ERK phosphorylation (Fig. 2F), and this inhibition was dose dependent (Fig. 2G). Trastuzumab did not have inhibitory effect on ERK phosphorylation in both cell lines (data not shown; Fig. 2F). These results indicate that coexpression of both high levels of HER2 and IGF-IR in cancer cells raise the bars for antibodies to interfere with the receptor phosphorylation and downstream signaling, especially when the ligand (IGF-I) is present. Trastuzumab was ineffective in inhibiting phosphorylation of Akt and ERK in both MCF-7 and SKOV-3 cells in the presence or absence of IGF-I. Bi-Ab, m590, and Comb were equally effective in inhibiting phosphorylation of Akt and ERK in MCF-7 cells in the absence of ligand (data not shown) and in inhibiting ligand-induced Akt phosphorylation in MCF-7 cells (Fig. 2D), but Bi-Ab was more effective than m590 and Comb in inhibiting ligand-induced ERK phosphorylation in MCF-7 cells (Fig. 2D), and more effective than Comb in inhibiting ERK phosphorylation in SKOV-3 cells in the absence of ligand (Fig. 2F).

Bi-Ab more effectively inhibits cancer cell proliferation than trastuzumab and m590 *in vitro*, and preserves ADCC activity

The attenuation of the PI3K/Akt and MAPK pathways by Bi-Ab prompted us to analyze the effects of Bi-Ab on cancer cell proliferation. Bi-Ab treatment effectively inhibited SKOV-3 cell proliferation *in vitro* (Fig. 3A). Notably, although Comb treatment showed enhanced inhibition of SKOV-3 proliferation compared with trastuzumab treatment alone, both treatment conditions were significantly less potent than Bi-Ab, especially at high antibody concentrations (over 25 μg/mL; Fig. 3A). M590 inhibited SKOV-3 cell proliferation, but its effect decreased sharply as m590 concentration decreased (Fig. 3A).

To investigate whether "knob" and "hole" mutations affected Fc-mediated effector function, we tested Bi-Ab for ADCC activity in a flow cytometry-based assay using SKOV-3 as target cells and healthy human PBMCs

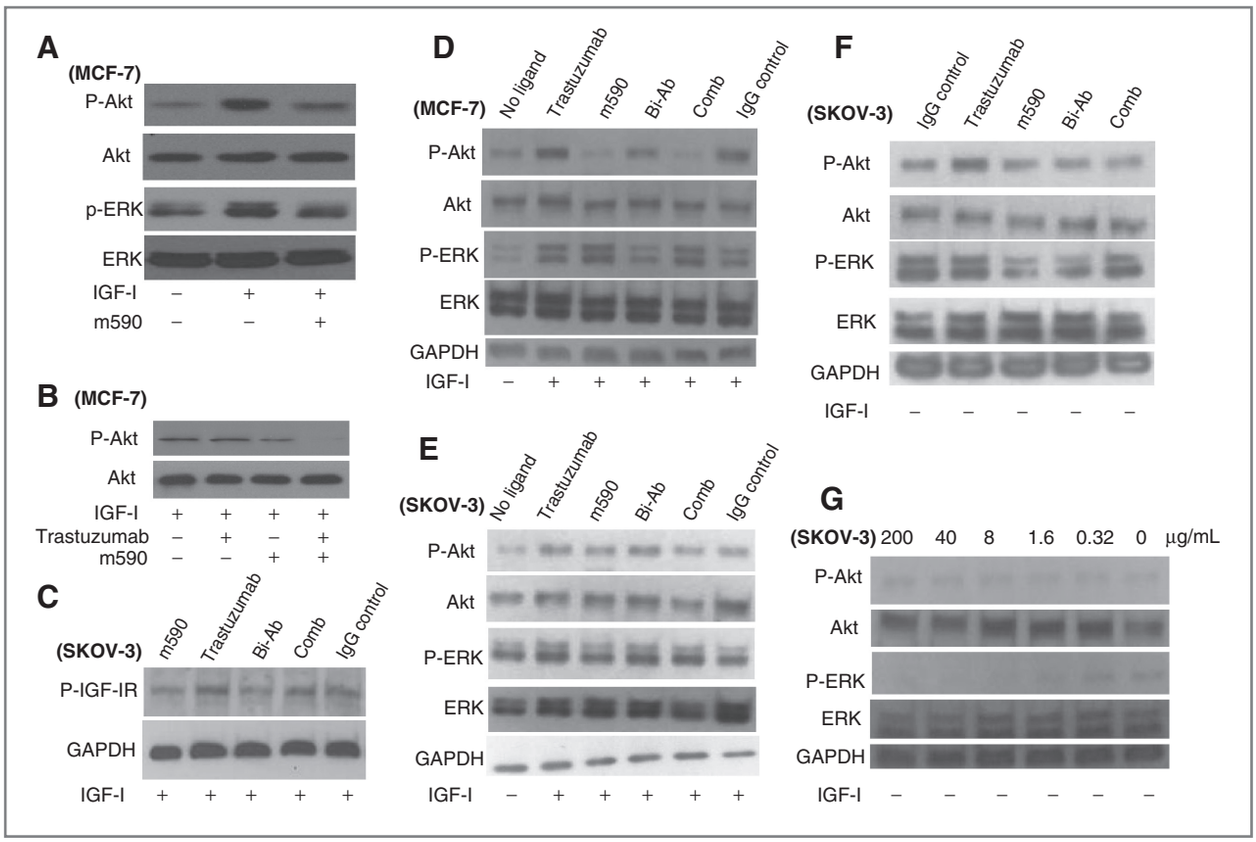

Figure 2. Inhibition of cancer cell signaling by Bi-Ab in comparison with m590 and trastuzumab alone, or in combination (Comb). A and B, inhibition of IGF-I (1.5 nmol/L) induced phosphorylation of Akt and ERK by m590 (40 nmol/L) alone (A) or in combination with trastuzumab (6.7 nmol/L; B) in MCF-7 cells. C, inhibition of IGF-I (1.5 nmol/L) induced phosphorylation of IGF-IR in SKOV-3 cells. D and E, inhibition of IGF-I (1.5 nmol/L) induced phosphorylation of Akt and ERK in MCF-7 (D) and SKOV-3 (E) cells. F, inhibition of phosphorylation of Akt and ERK by the antibodies in SKOV-3 cells in the absence of IGF-I. All antibodies were tested at 100 μg/mL and incubated with cells for 24 hours (C–F). G, dose-dependent inhibition of ERK phosphorylation, but not Akt phosphorylation by Bi-Ab in SKOV-3 cells in the absence of IGF-I. Bi-Ab: 200, 40, 8, 1.6, 0.32, and 0 μg/mL.

as effector cells. The assay revealed that Bi-Ab had ADCC activity comparable with or slightly higher than that of m590, trastuzumab, and the combination of m590 and trastuzumab (Comb; Fig. 3B). Notably, percentage of ADCC with Bi-Ab was significantly higher than that with Comb at 1 μg/mL ($P < 0.05$). These results suggest that Bi-Ab remains effective in killing HER2- and/or IGF-IR–overexpressing tumor cells through ADCC *in vivo*.

Bi-Ab inhibits tumor growth in SKOV-3 HER2- and IGF-IR–overexpressing xenograft mouse model

To establish a HER2- and IGF-IR–overexpressing cancer xenograft mouse model for testing the effect of Bi-Ab *in vivo*, we generated a SKOV-3-Luc stable cell line expressing luciferase. We tested Bi-Ab, m590, trastuzumab, and Comb in this mouse model following the protocol shown in Fig. 4A. There were a total of four experimental groups, and each group had seven nude mice. A control group that had five nude mice was included in the study. Three million of SKOV-3-Luc cells were injected subcutaneously to each nude mouse, and antibodies (100 μg per mouse) were injected intraperitoneally on days 1, 4, 6, and 8 postinoculations. Mouse body weight and luminescence intensity in the ROI were measured on days 1, 4, 6, and 8 before antibody injections, and repeated on days 11, 15, 25, and 35 postinoculations. The average body weight of Bi-Ab–treated mice did not decrease throughout the study, whereas the average mouse body weight of the other three experimental groups decreased on day 4. Nevertheless, there was no significant difference in average body weight among the four groups at comparable time points (data not shown).

The average luminescence intensities varied across all the experimental groups (Fig. 4B). Notably, the Bi-Ab–treated group experienced a dramatic inhibition of tumor growth that lasted for a much longer time compared with the other three groups. The Bi-Ab group showed significantly lower average luminescence intensities than the m590 group ($P < 0.001$) from day 6 to day 35, the end of the mouse study, whereas the Comb group only showed significantly lower average luminescence intensities than the m590 group on days 6, 8, and 11, and the trastuzumab group only showed

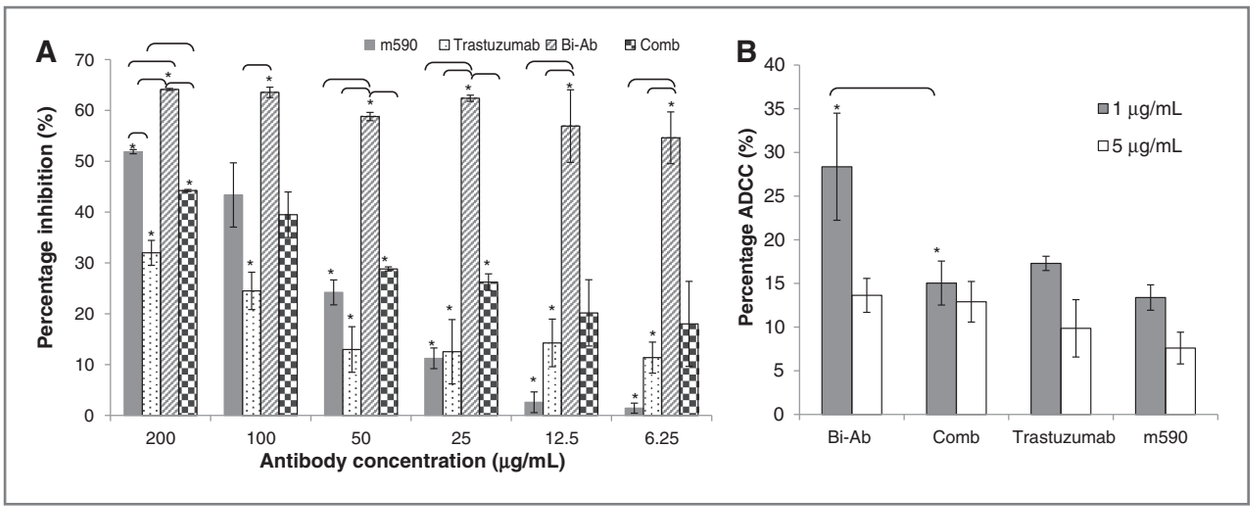

Figure 3. Characterization of Bi-Ab for inhibitory activity in SKOV-3 cell proliferation and ADCC activity in comparison with m590 and trastuzumab alone, or in combination (Comb). A, inhibition of SKOV-3 cell proliferation in MTT assay. Percentage of inhibition at each antibody concentration was used in one-way ANOVA statistical analysis to test whether there was significant difference between any two antibodies at the same concentration. Two paired antibodies with significant difference (*, $P < 0.001$) in percentage of inhibition are indicated. B, percentage of ADCC of the antibodies at 1 and 5 μg/mL. The same ANOVA statistical analysis was done to test whether there was significant difference in percentage of ADCC between any two antibodies at the same concentration. Percentage of ADCC between Bi-Ab and Comb at 1 μg/mL showed significant difference (*, $P < 0.05$), which is indicated. Each antibody dilution was tested in triplicate and the assays were repeated once.

significant lower average luminescence intensities than the m590 group on days 8 and 11 (Fig. 5A). The average luminescence intensity of the m590 group also decreased on day 11, and further decreased on day 15, but returned to high levels on days 25 and 35. These decreases may not be caused by m590 treatment because the control group also showed slightly decreases in average luminescence intensity on day 11 and 15 (Fig. 4B). The Comb group showed relapse (increased average luminescence intensity) starting on day 25, whereas the trastuzumab group relapsed earlier on day 15. The average luminescence intensity of the Bi-Ab on day 35 slightly increased, but it was still significantly lower than that of the m590 group (Fig. 5A).

We then investigated individual mouse in each group and counted the number of mouse that had 2-fold higher luminescence intensity than the baseline level (no inoculation; Fig. 5B). The Bi-Ab group showed early decrease in luminescence intensity. Five out seven mice in the Bi-Ab group had luminescence intensities below 2-fold of the baseline level on day 4, whereas only three out of seven mice in the Comb and trastuzumab groups had the same low levels of luminescence intensity on day 4 (Fig. 5B). The rest two mice in the Bi-Ab showed luminescence intensities below 2-fold of the baseline level on days 8 and 15, and the luminescence intensities of all mice in the Bi-Ab group remained low till the end of the mouse study except that one mouse relapsed on day 35 (Fig. 5B). Five out of seven mice in the Comb group showed luminescence intensities below 2-fold of the baseline level on days 6 and 8, but one of these five mice in the Comb group relapsed on day 35. Six out of seven mice in the trastuzumab group showed luminescence intensities below 2-fold of the baseline level on day 8, but these mice relapsed one by one as the study progressed. There was only one mouse left in the trastuzumab group that had the luminescence intensity below 2-fold of the baseline level on day 35 (Fig. 5B). None of mice in the m590 ever exhibited luminescence intensity below 2-fold of the baseline level throughout the study. These results indicate that dual targeting HER2 and IGF-IR is more effective than single targeting in inhibiting HER2- and IGF-IR–overexpressing tumor growth and postponing tumor relapse *in vivo*, and Bi-Ab more effectively inhibits tumor growth and prevents tumor relapse than simple combination of two monospecific antibodies.

Discussion

Breast cancer is one of the most common cancers in women. It accounts for 22.9% of all cancer cases in women worldwide and was responsible for 13.7% of cancer deaths in 2008. EGFR and IGF-IR activation contributes to the initiation and progression of breast cancer. Trastuzumab (trastuzumab) has been in clinical use for treatment of HER2-overexpressing breast cancers, but patients often develop resistance to the therapy. Thus, there is a need for novel therapies. In this study, we generated and tested Bi-Ab, a "knobs-into-holes" Bi-Ab that cotargets HER2 and IGF-IR, in *in vitro* assays and in the tumor xenograft mouse model overexpressing both HER2 and IGF-IR. Our results indicate that cotargeting HER2 and IGF-IR may be of clinical relevance in treating HER2- and/or IGF-IR–overexpressing human cancers.

This study was promoted by our observation that m590 synergized with trastuzumab in inhibiting Akt phosphorylation in MCF-7 cells (Fig. 2B). But when we

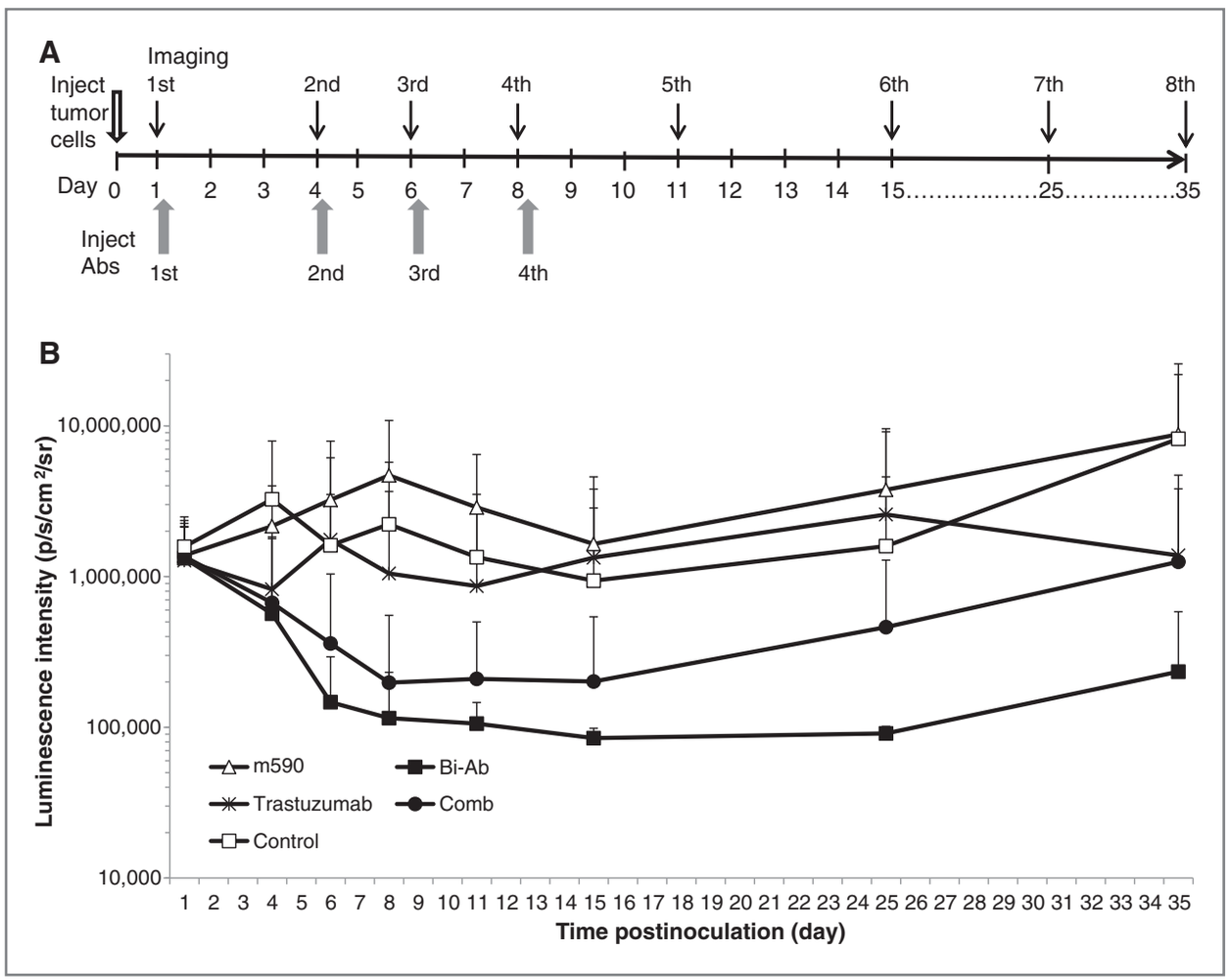

Figure 4. Diagram of the mouse study and tumor growth kinetics in each group of mice treated with or without antibodies (control). A, diagram of the mouse study. Three million of SKOV-3-Luc cells were injected subcutaneously into each nude mouse on day 0. 100 μg of Bi-Ab, or m590, or trastuzumab, or Comb were injected intraperitoneally on day 1, 4, 6, and 8 postinoculations. Mouse imaging was performed on day 1, 4, 6, and 8 before antibody injections, and on day 11, 15, 25, and 35 postinoculations. Seven mice were included in each antibody-treated group, but only five mice were in the control group. B, average luminescence intensity in each group of mice at different time point. Logarithmic values of the average luminescence intensities and standard variations were shown.

come to SKOV-3 cell line that expresses much higher level of HER2 than MCF-7, the inhibition of Akt and ERK phosphorylation by antibodies becomes complicated. This may attribute to two reasons. First, anti-HER2 mAb trastuzumab downregulates the phosphorylation of Ras, Raf, MAP–ERK kinase, and MAPK (ERK; ref. 6). ERK kinase can phosphorylate dual specific phosphatases Cdc25c. Downregulated ERK phosphorylation reduces the activity of Cdc25c, resulting in increased phosphorylation of RTK, such as IGF-IR. Therefore, although the MAPK pathway is blocked by trastuzumab, following the activation of IGF-IR, the PI3K/Akt pathway is triggered, leading to a compensatory effect, which rescues tumor cells from apoptosis. This feedback loop was first reported by Prahallad and colleagues (45). We observed the same phenomenon in this study (Fig. 2D–F). The increased Akt phosphorylation caused by the feedback loop makes anti-IGF-IR mAb m590 less effective in inhibiting Akt phosphorylation, especially in the presence of IGF-I (Fig. 2E and F). Nevertheless, m590 and Bi-Ab inhibit ligand-induced phosphorylation of IGF-IR in SKOV-3 cells (Fig. 2F), and Bi-Ab inhibits ERK phosphorylation in a dose-dependent manner in SKOV-3 cells in the absence of IGF-I (Fig. 2G). Second, high levels of HER2 and IGF-IR in SKOV-3 cells may promote the formation of HER2/IGF-IR heterodimer. Indeed, Browne and colleagues reported the existence of HER2/IGF-IR complexes in trastuzumab-resistant breast cancer SKBR3 cells and found that cotargeting both receptors improved the efficacy of trastuzumab *in vitro* (37). HER2/IGF-IR heterodimer may be less sensitive to monospecific antibodies, trastuzumab and m590. To inhibit the signaling of HER2/IGF-IR heterodimer, Bi-Ab is expected to be more effective than Comb because there may be steric hindrance when

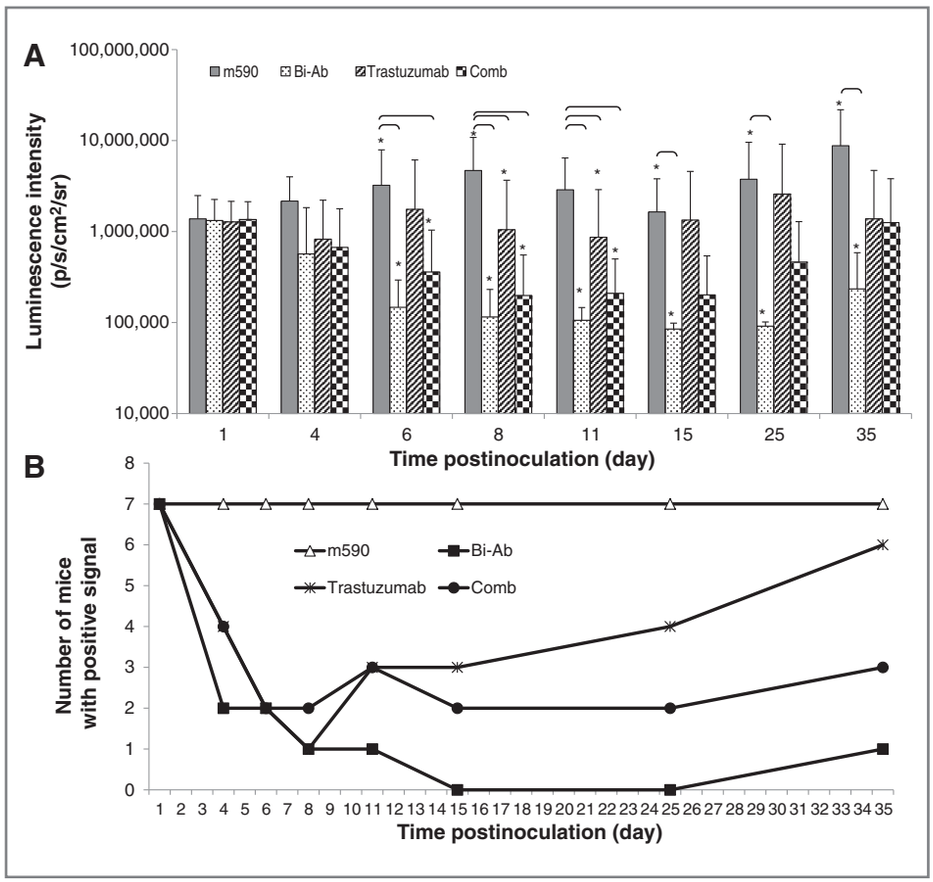

Figure 5. Inhibition of cancer growth by Bi-Ab in SKOV-3 HER2- and IGF-IR–overexpressing xenograft mouse model in comparison with m590 and trastuzumab alone, or in combination (Comb). A, average luminescence intensity in each group of mice at different time point. Logarithmic values of the average luminescence intensity were used in ANOVA statistical analysis to test whether there was significant difference between any two groups at the same time point. Two paired groups with significant difference (*, $P < 0.001$) are indicated. B, number of mice in each group with luminescence intensity 2-fold higher than the baseline level.

two IgG molecules need to bind simultaneously to the same heterodimer. This may be one of the reasons why Bi-Ab is more effective than Comb in inhibiting cancer cell proliferation *in vitro* and tumor growth in the tumor xenograft mouse model.

Different methodologies have been described to generate bispecific antibodies by design (42, 46). We took advantage of the "knobs-into-holes" strategy for generating Bi-Ab (42). Cotransfection of 293F cells with the "knob" and "hole" mutant plasmids yielded Bi-Ab. Protein A affinity-purified Bi-Ab showed a single peak in gel filtration (data not shown). More importantly, "knobs-into-holes" mutations located in the CH3 domain did not affect antibody effector functions, which are mediated mainly by the CH2 domain of antibodies as evidenced by the high ADCC activity of Bi-Ab. ADCC is an important mechanism of action for therapeutic antibodies *in vivo* (47–49). The result from our ADCC assay demonstrates that Bi-Ab has comparable or slightly enhanced ADCC activity compared with monospecific antibodies, m590 and trastuzumab, and the Comb. Notably, this is the first report showing that the "knobs-into-holes" strategy did not affect ADCC activity of the resultant Bi-Ab. Nude mice have relatively normal natural killer (NK) cells and human IgG1 can bind to mouse Fc-γ receptor III (FcrRIII, CD16) on NK cells. Thus, administration of human IgG1s or human/mouse chimeric antibodies into mice can induce ADCC and Ab-dependent cellular phagocytosis in NK cells, polymorphonuclear leukocytes, and macrophages (50). Both trastuzumab and m590 contain human IgG1 Fc, therefore, the inhibitory effect observed in this mouse study may result from Fab-mediated direct effects of the antibodies and Fc-mediated ADCC and phagocytosis.

In the current mouse study, tumor growth was more effectively inhibited by Bi-Ab than trastuzumab and Comb. Out of seven mice in each experimental group, six mice in the Bi-Ab group were still having low luminescence intensities (below 2-fold of the baseline level) in the end of the study (day 35 postinoculations of SKOV-3-Luc cells), whereas this number was four in the Comb group and one in the trastuzumab group. Although m590 alone failed to bring the luminescence intensity to such low level, coadministration of m590 with trastuzumab (Comb) significantly enhanced the inhibitory effect of trastuzumab. Cotargeting IGF-IR– and HER2-overexpressing tumor xenografts with Bi-Ab worked even better than the simple mixture of two monospecific antibodies (Comb), which may be ascribed to the more effective inhibition of ERK phosphorylation and ligand-induced IGF-IR phosphorylation by Bi-Ab in SKOV-3 cells (Fig. 2C and D), and enhanced ADCC activity of Bi-Ab compared with Comb. These results indicate that Bi-Ab has superior antitumor activity compared with the monospecific antibodies alone or in combination, and cotargeting HER2 and

IGF-IR with Bi-Ab may be clinically beneficial in minimizing the acquired resistance to the current trastuzumab therapy.

Disclosure of Potential Conflicts of Interest

No potential conflicts of interest were disclosed.

Authors' Contributions

Conception and design: C. Chen, S.W. Tsao, M.-Y. Zhang
Development of methodology: C. Chen, Y. Zhang, M.-Y. Zhang
Acquisition of data (provided animals, acquired and managed patients, provided facilities, etc.): C. Chen
Analysis and interpretation of data (e.g., statistical analysis, biostatistics, computational analysis): C. Chen, Y. Zhang, M.-Y. Zhang
Writing, review, and/or revision of the manuscript: C. Chen, M.-Y. Zhang
Administrative, technical, or material support (i.e., reporting or organizing data, constructing databases): C. Chen, Y. Zhang, J. Li
Study supervision: M.-Y. Zhang

Acknowledgments

The authors thank Zhiwei Chen and Li Liu for providing the recombinant plasmids containing luciferase and Gag-pol genes, Hong Zheng (Huazhong University of Science and Technology, Wuhan, China) for providing the data shown in Fig. 2A and B, Vikram Srivastava and Zhiwu Tan for helpful discussions; and Man-Chung Yeung for technical assistance.

Grant Support

This work was supported by Hong Kong Innovation and Technology Fund (ITS106/11) to M.-Y. Zhang.

The costs of publication of this article were defrayed in part by the payment of page charges. This article must therefore be hereby marked *advertisement* in accordance with 18 U.S.C. Section 1734 solely to indicate this fact.

Received July 17, 2013; revised October 15, 2013; accepted October 30, 2013; published OnlineFirst November 13, 2013.

References

1. Herbst RS. Review of epidermal growth factor receptor biology. Int J Radiat Oncol Biol Phys 2004;59:21–6.
2. Olayioye MA. Update on HER-2 as a target for cancer therapy: intracellular signaling pathways of ErbB2/HER-2 and family members. Breast Cancer Res 2001;3:385–9.
3. Spivak-Kroizman T, Rotin D, Pinchasi D, Ullrich A, Schlessinger J, Lax I. Heterodimerization of c-erbB2 with different epidermal growth factor receptor mutants elicits stimulatory or inhibitory responses. J Biol Chem 1992;267:8056–63.
4. Ferguson KM, Berger MB, Mendrola JM, Cho HS, Leahy DJ, Lemmon MA. EGF activates its receptor by removing interactions that autoinhibit ectodomain dimerization. Mol Cell 2003;11:507–17.
5. Garrett TP, McKern NM, Lou M, Elleman TC, Adams TE, Lovrecz GO, et al. The crystal structure of a truncated ErbB2 ectodomain reveals an active conformation, poised to interact with other ErbB receptors. Mol Cell 2003;11:495–505.
6. Stern HM. Improving treatment of HER2-positive cancers: opportunities and challenges. Sci Transl Med 2012;4:127rv2.
7. Liu X, Fridman JS, Wang Q, Caulder E, Yang G, Covington M, et al. Selective inhibition of ADAM metalloproteases blocks HER-2 extracellular domain (ECD) cleavage and potentiates the anti-tumor effects of trastuzumab. Cancer Biol Ther 2006;5:648–56.
8. Lane HA, Beuvink I, Motoyama AB, Daly JM, Neve RM, Hynes NE. ErbB2 potentiates breast tumor proliferation through modulation of p27(Kip1)-Cdk2 complex formation: receptor overexpression does not determine growth dependency. Mol Cell Biol 2000;20:3210–23.
9. Dankort D, Jeyabalan N, Jones N, Dumont DJ, Muller WJ. Multiple ErbB-2/Neu phosphorylation sites mediate transformation through distinct effector proteins. J Biol Chem 2001;276:38921–8.
10. Abu Hejleh T, Deyoung BR, Engelman E, Deutsch JM, Zimmerman B, Halfdanarson TR, et al. Relationship between HER-2 overexpression and brain metastasis in esophageal cancer patients. World J Gastrointest Oncol 2012;4:103–8.
11. Geng Y, Wang J, Wang R, Wang K, Xu Y, Song G, et al. Leptin and HER-2 are associated with gastric cancer progression and prognosis of patients. Biomed Pharmacother 2012;66:419–24.
12. Nanni P, Nicoletti G, Palladini A, Croci S, Murgo A, Ianzano ML, et al. Multiorgan metastasis of human HER-2(+) breast cancer in Rag2(−)/(−);Il2rg(−)/(−) mice and treatment with PI3K inhibitor. PLoS ONE 2012;7:e39626.
13. Ravdin PM, Chamness GC. The c-erbB-2 proto-oncogene as a prognostic and predictive marker in breast cancer: a paradigm for the development of other macromolecular markers–a review. Gene 1995;159:19–27.
14. Slamon DJ, Clark GM, Wong SG, Levin WJ, Ullrich A, McGuire WL. Human breast cancer: correlation of relapse and survival with amplification of the HER-2/neu oncogene. Science 1987;235:177–82.
15. Slamon DJ, Godolphin W, Jones LA, Holt JA, Wong SG, Keith DE, et al. Studies of the HER-2/neu proto-oncogene in human breast and ovarian cancer. Science 1989;244:707–12.
16. Jones JI, Clemmons DR. Insulin-like growth factors and their binding proteins: biological actions. Endocr Rev 1995;16:3–34.
17. LeRoith D, Werner H, Beitner-Johnson D, Roberts CT Jr. Molecular and cellular aspects of the insulin-like growth factor I receptor. Endocr Rev 1995;16:143–63.
18. Warshamana-Greene GS, Litz J, Buchdunger E, Garcia-Echeverria C, Hofmann F, Krystal GW. The insulin-like growth factor-I receptor kinase inhibitor, NVP-ADW742, sensitizes small cell lung cancer cell lines to the effects of chemotherapy. Clin Cancer Res 2005;11:1563–71.
19. Jones HE, Goddard L, Gee JM, Hiscox S, Rubini M, Barrow D, et al. Insulin-like growth factor-I receptor signalling and acquired resistance to gefitinib (ZD1839; Iressa) in human breast and prostate cancer cells. Endocr Relat Cancer 2004;11:793–814.
20. Krueckl SL, Sikes RA, Edlund NM, Bell RH, Hurtado-Coll A, Fazli L, et al. Increased insulin-like growth factor I receptor expression and signaling are components of androgen-independent progression in a lineage-derived prostate cancer progression model. Cancer Res 2004;64:8620–9.
21. Yao H, Dashner EJ, van Golen CM, van Golen KL. RhoC GTPase is required for PC-3 prostate cancer cell invasion but not motility. Oncogene 2006;25:2285–96.
22. Hudis CA. Trastuzumab–mechanism of action and use in clinical practice. N Engl J Med 2007;357:39–51.
23. Tokunaga E, Oki E, Nishida K, Koga T, Egashira A, Morita M, et al. Trastuzumab and breast cancer: developments and current status. Int J Clin Oncol 2006;11:199–208.
24. Cuello M, Ettenberg SA, Clark AS, Keane MM, Posner RH, Nau MM, et al. Down-regulation of the erbB-2 receptor by trastuzumab (herceptin) enhances tumor necrosis factor-related apoptosis-inducing ligand-mediated apoptosis in breast and ovarian cancer cell lines that overexpress erbB-2. Cancer Res 2001;61:4892–900.
25. Albanell J, Codony J, Rovira A, Mellado B, Gascon P. Mechanism of action of anti-HER2 monoclonal antibodies: scientific update on trastuzumab and 2C4. Adv Exp Med Biol 2003;532:253–68.
26. Molina MA, Codony-Servat J, Albanell J, Rojo F, Arribas J, Baselga J. Trastuzumab (herceptin), a humanized anti-Her2 receptor monoclonal antibody, inhibits basal and activated Her2 ectodomain cleavage in breast cancer cells. Cancer Res 2001;61:4744–9.
27. Clynes RA, Towers TL, Presta LG, Ravetch JV. Inhibitory Fc receptors modulate *in vivo* cytotoxicity against tumor targets. Nat Med 2000;6:443–6.

28. Nahta R, Shabaya S, Ozbay T, Rowe DL. Personalizing HER2-targeted therapy in metastatic breast cancer beyond HER2 status: what we have learned from clinical specimens. Curr Pharmacogenomics Person Med 2009;7:263–74.

29. Nahta R, Yu D, Hung MC, Hortobagyi GN, Esteva FJ. Mechanisms of disease: understanding resistance to HER2-targeted therapy in human breast cancer. Nat Clin Pract Oncol 2006;3:269–80.

30. Yarden Y, Sliwkowski MX. Untangling the ErbB signalling network. Nat Rev Mol Cell Biol 2001;2:127–37.

31. Huang X, Gao L, Wang S, McManaman JL, Thor AD, Yang X, et al. Heterotrimerization of the growth factor receptors erbB2, erbB3, and insulin-like growth factor-i receptor in breast cancer cells resistant to herceptin. Cancer Res 2010;70:1204–14.

32. Nahta R, Yuan LX, Zhang B, Kobayashi R, Esteva FJ. Insulin-like growth factor-I receptor/human epidermal growth factor receptor 2 heterodimerization contributes to trastuzumab resistance of breast cancer cells. Cancer Res 2005;65:11118–28.

33. Jin Q, Esteva FJ. Cross-talk between the ErbB/HER family and the type I insulin-like growth factor receptor signaling pathway in breast cancer. J Mammary Gland Biol Neoplasia 2008;13:485–98.

34. Bender LM, Nahta R. Her2 cross talk and therapeutic resistance in breast cancer. Front Biosci 2008;13:3906–12.

35. Casa AJ, Dearth RK, Litzenburger BC, Lee AV, Cui X. The type I insulin-like growth factor receptor pathway: a key player in cancer therapeutic resistance. Front Biosci 2008;13:3273–87.

36. Lu Y, Zi X, Zhao Y, Mascarenhas D, Pollak M. Insulin-like growth factor-I receptor signaling and resistance to trastuzumab (Herceptin). J Natl Cancer Inst 2001;93:1852–7.

37. Browne BC, Crown J, Venkatesan N, Duffy MJ, Clynes M, Slamon D, et al. Inhibition of IGF1R activity enhances response to trastuzumab in HER-2-positive breast cancer cells. Ann Oncol 2011;22:68–73.

38. Harris LN, You F, Schnitt SJ, Witkiewicz A, Lu X, Sgroi D, et al. Predictors of resistance to preoperative trastuzumab and vinorelbine for HER2-positive early breast cancer. Clin Cancer Res 2007;13:1198–207.

39. Zhang MY, Feng Y, Wang Y, Dimitrov DS. Characterization of a chimeric monoclonal antibody against the insulin-like growth factor-I receptor. MAbs 2009;1:475–80.

40. Srivastava V, Yang Z, Hung IF, Xu J, Zheng B, Zhang MY. Identification of dominant antibody-dependent cell-mediated cytotoxicity epitopes on the hemagglutinin antigen of pandemic H1N1 influenza virus. J Virol 2013;87:5831–40.

41. Ridgway JB, Presta LG, Carter P. 'Knobs-into-holes' engineering of antibody CH3 domains for heavy chain heterodimerization. Protein Eng 1996;9:617–21.

42. Carter P. Bispecific human IgG by design. J Immunol Methods 2001;248:7–15.

43. Atwell S, Ridgway JB, Wells JA, Carter P. Stable heterodimers from remodeling the domain interface of a homodimer using a phage display library. J Mol Biol 1997;270:26–35.

44. Fu X-Y, Chen C, Pan H-X, Zhou B, Li W-Y, Huang T, et al. Inhibition of breast cancer cell proliferation and migration by monoclonal antibody m590 specific for insulin-like growth factor receptor type I. Chin J Exp Surg 2012;29:824–6.

45. Prahallad A, Sun C, Huang S, Di Nicolantonio F, Salazar R, Zecchin D, et al. Unresponsiveness of colon cancer to BRAF(V600E) inhibition through feedback activation of EGFR. Nature 2012;483:100–3.

46. Carter PJ. Potent antibody therapeutics by design. Nat Rev Immunol 2006;6:343–57.

47. Musolino A, Naldi N, Bortesi B, Pezzuolo D, Capelletti M, Missale G, et al. Immunoglobulin G fragment C receptor polymorphisms and clinical efficacy of trastuzumab-based therapy in patients with HER-2/neu-positive metastatic breast cancer. J Clin Oncol 2008;26:1789–96.

48. Zhang W, Gordon M, Schultheis AM, Yang DY, Nagashima F, Azuma M, et al. FCGR2A and FCGR3A polymorphisms associated with clinical outcome of epidermal growth factor receptor expressing metastatic colorectal cancer patients treated with single-agent cetuximab. J Clin Oncol 2007;25:3712–8.

49. Hessell AJ, Hangartner L, Hunter M, Havenith CE, Beurskens FJ, Bakker JM, et al. Fc receptor but not complement binding is important in antibody protection against HIV. Nature 2007;449:101–4.

50. Overdijk MB, Verploegen S, Ortiz Buijsse A, Vink T, Leusen JH, Bleeker WK, et al. Crosstalk between human IgG isotypes and murine effector cells. J Immunol 2012;189:3430–8.